Available online at www.sciencedirect.com
ScienceDirect
Thin Solid Films 515 (2007) 5852–5856
www.elsevier.com/locate/tsf

Comparative study of sputtered and electrodeposited CI(S,Se) and CIGSe thin films

A. Ihlal [a,*], K. Bouabid [a], D. Soubane [a,c], M. Nya [a], O. Ait-Taleb-Ali [a], Y. Amira [a], A. Outzourhit [b], G. Nouet [c]

[a] Laboratoire Matériaux et Energies Renouvelables (LMER), Faculté des Sciences, BP 8106, Hay Dakhla, Agadir, Maroc
[b] Laboratoire de Physique des Solides et des Couches Minces (LPSCM), Département de physique, Faculté des sciences Semlalia, BP: S/3293, Marrakech, Maroc
[c] Structure des Interfaces et Fonctionnalité des couches minces (SIFCOM), Ensicaen, Bd du Maréchal Juin, 14050 Caen, France

Available online 24 January 2007

Abstract

Copper indium disulphide $CuInS_2$ (CIS) and diselenide $CuInSe_2$ (CISe) and their alloys with gallium $CuIn_{1-x}Ga_xSe_2$ (CIGSe) thin films have been prepared using both high- and non-vacuum processes. The well known two-stage process consisting in a sequential sputtering of Cu and In thin layers and a subsequent sulfurisation has led to the formation of good quality $CuInS_2$ ternary compound. The films exhibit the well known chalcopyrite structure with a preferential orientation in the (112) plane suitable for the production of the efficient solar cells. The absorption coefficient of the films is higher than 10^4 cm^{-1} and the band gap value is about 1.43 eV. A non-vacuum technique was also used. It consists on a one step electrodeposition of Cu, In and Se and in a second time Cu, In, Se and Ga. From the morphological and structural point of view, the films obtained are similar to those prepared by the first technique. The band gap value increases up from 1 eV for the CIS films to 1.26 eV for the $CuIn_{1-x}Ga_xSe_2$ with $0<x<0.23$. The resistivity at room temperature of the films was adjusted to 10 Ωcm after annealing. The films exhibit an absorption coefficient more than 10^5 cm^{-1}. The most important conclusion of this study is the interesting potential of electrodeposition as a promising option in low-cost CISe and CIGSe thin film based solar cells processing.

Keywords: CI(S,Se); CIGSe; Electrodeposition; rf-sputtering; Sulfurisation

1. Introduction

Because of their high absorption coefficient of sun light and their high tolerance to the presence of defects (grain boundaries, vacancies, interstitials...), ternary chalcopyrite, CI(S,Se) and their alloys with gallium CIG(S,Se) are becoming among the leading candidates for high efficiency and low-cost terrestrial photovoltaic devices. Indeed, polycrystalline CI(S,Se) and CIG(S,Se) based solar cells have achieved efficiencies of about 19% on a laboratory scale [1–3] and around 14% for modules [4]. Furthermore, the cells have shown very good outdoor stability and resistance to radiations [5]. CI(S,Se) and CIG(S,Se) thin films have been prepared using a variety of processes including coevaporation of the elements in different ways [3,6–8], two or three stage process consisting in sequentially sputtered Cu and In thin layers and a subsequent chalcogenisation by selenisation [9,10], and electrodeposition [11–13]. The properties of the grown layers seem to be dependent on the preparation technique. The best results were obtained by the coevaporation process [3]. However, it is difficult in upscaling and involves high vacuum and thus high cost. Though electrodeposition has led to the preparation of conversion structures with efficiency less than its counterpart vacuum techniques, it is a very attractive technique because it is cost effective and suitable for large area modules and thus constitutes a possible alternative to decrease the production costs of CI(S,Se) and CIG(S,Se) modules. Finally, CdS was the buffer layer currently used in chalcopyrite based solar cells. However, Cadmium is a heavy metal and should be avoided. Alternative buffer layers were developed such as Zn(X,O) (X=S, Se) [14,15], In(OH,S) [16], ZnS [17], In_2S_3 [18,19]. Such a reduction of environmental

* Corresponding author.
E-mail address: ihlal_ahmed@yahoo.fr (A. Ihlal).

0040-6090/$ - see front matter © 2006 Elsevier B.V. All rights reserved.
doi:10.1016/j.tsf.2006.12.136

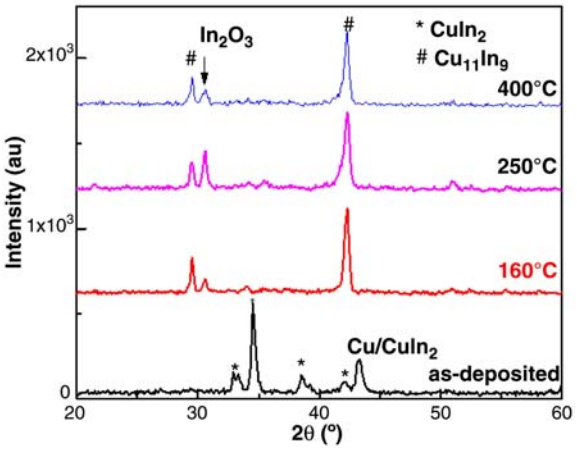

Fig. 1. XRD patterns of as-deposited and annealed Cu–In multilayers at 160, 250 and 400 °C in vacuum.

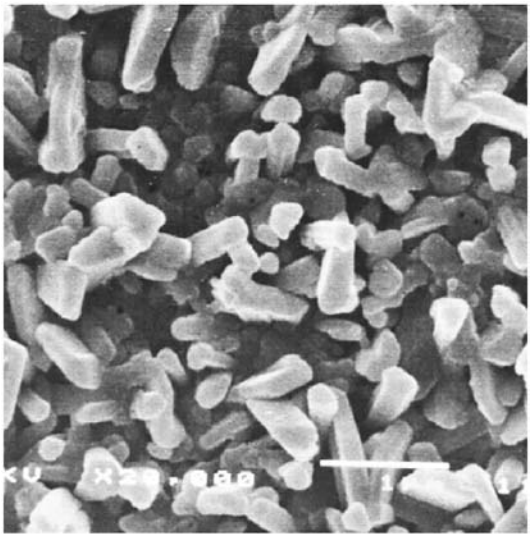

Fig. 3. SEM micrograph of a sulfurised Cu–In multilayer at 400 °C.

impact will significantly foster the development of CI(S,Se) technology. The present contribution deals with a comparative study of structural, optical and electrical properties of CIS, CISe and CIGSe thin films grown by both a vacuum and a non-vacuum method. A two-stage growth process consisting on a sequential deposition by sputtering of Cu and In layers on Mo coated glass and a subsequent sulfurisation of this multilayer structure in vacuum partial pressure, and a non-vacuum process consisting in one step electrodeposition of the elements.

2. Experimental details

2.1. Preparation of $CuInS_2$ (CIS) films

Cu–In metallic precursor multilayers were obtained by rf sputtering technique. Sequential deposition of Cu and In were performed on Mo coated glass substrates. Altogether 20 alternate layers were obtained under a 2×10^{-5} Torr partial argon pressure. The thickness of the samples was varied by increasing the deposition time from 5 to 20 min per layer. All the samples were subsequently annealed at temperatures scaling from 160 to 400 °C for 2 h in vacuum (10^{-3} Torr). The samples were inserted then into a partially closed quartz tube containing sulphur. The tube was then introduced in a furnace. The process of sulfurisation was realized at temperatures scaling from 160 to 400 °C during 20 h under a vacuum partial pressure of about 10^{-3} Torr.

2.2. Electrodeposition of $CuInSe_2$ (CISe) and $CuIn_{1-x}Ga_xSe_2$ (CIGSe)

The principle of this technique for the preparation of CI(S, Se) and CIG(S,Se) thin films have been exposed and extensively discussed by Lincot et al. [13]. In our case, CISe and CIGSe thin films were deposited onto Mo coated glass adopting potentiostatic electrochemical method. The complete route was described in our previous work [11,20,21]. The electrolyte bath consisted in $CuSO_4$ (2.5–3.5 mM), $In_2(SO_4)_3$ (2–3.5 mM) and SeO_2 (5 mM). For CIGSe thin film deposition, $Ga_2(SO_4)_3$ (0–2.5 mM) was added in different amount for Ga grading. Citric acid ($C_6H_8O_7$, H_2O), with a concentration between 0.1 and 0.3 M, was used as a complexing agent.

The samples obtained were then heat treated and characterised. The structure of the films was determined by means of X-ray

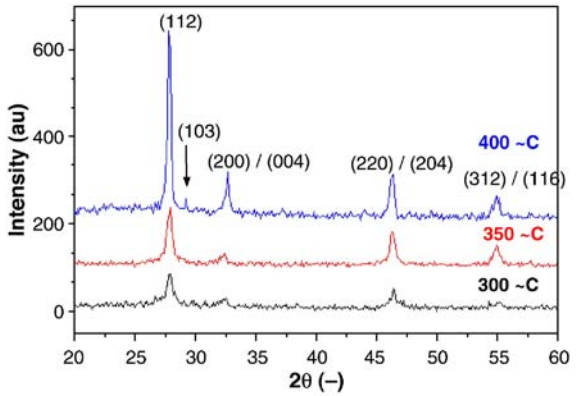

Fig. 2. XRD patterns of sulfurised Cu–In multilayers at 300, 350 and 400 °C.

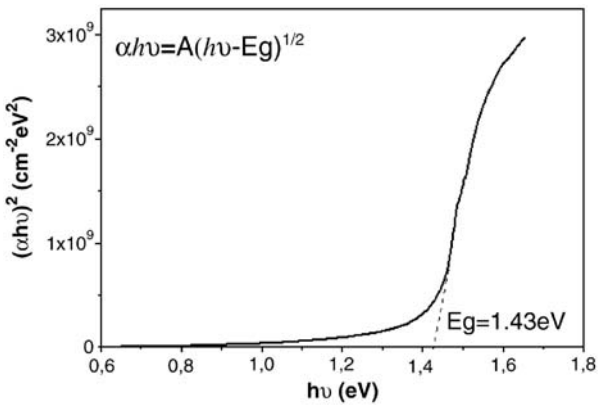

Fig. 4. Plots of $(\alpha h\upsilon)^2$ versus hυ for the film sulfurised at 400 °C.

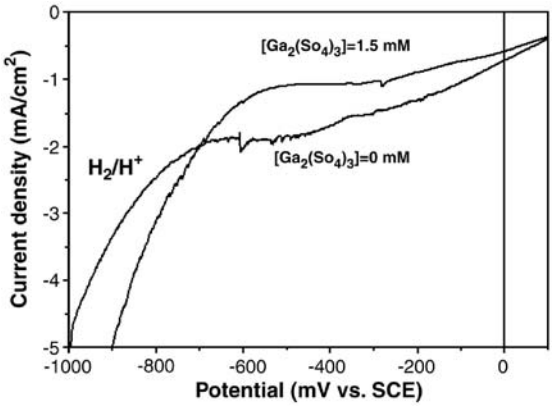

Fig. 5. Voltamograms of a solution containing CuSO4 3 mM, In2(SO4)3 3 mM, SeO2 5 mM and Ga2(SO4)3 1.5 mM. Note that the vigorous evolution of the current for potentials below −700 mV vs. SCE is due to Hydrogen and no proper deposition could be obtained.

diffraction (XRD) using a Phillips PW 1840 diffractometer and a scanning electron microscope (SEM) Jeol 5500. The composition of the films was determined by means of energy dispersive X-ray (EDS) microanalyser. The optical characteristics were determined at normal incidence in the wavelength range 320 to 3200 nm using a Shimadzu UV-3101 PC spectrophotometer.

3. Results and discussions

3.1. Sulfurised Cu–In multilayers

In order to understand the sulfurisation mechanism of our Cu–In multilayers with the annealing temperature, XRD analyses were performed to identify the formation of different phases. Fig. 1 shows the XRD spectra of Cu–In multilayers before sulfurisation. Cu and Cu–In alloy ($CuIn_2$) are detected but indium cannot be observed. The formation of $CuIn_2$ compound during the deposition was reported by other authors [9,22]. Annealing at 160, 250 and 400 °C lead to the formation of the $Cu_{11}In_9$ phase and the existence of a peak characterizing the indium oxide (In_2O_3). The adsorption of oxygen on our samples should have occurred during the transfer from the sputtering reactor to the furnace for heat treatments.

Fig. 2 shows the XRD spectra of the sulfurised layers during 20 h at different temperatures. The peaks (112), (220)/(204) and (312) are characteristic of the chalcopyrite and sphalerite structures in good agreement with the results reported by other authors [9,23]. The presence of the peak (103) after sulfurisation at 400 °C indicates the formation of the chalcopyrite structure. The salient feature of these spectra is the preferential orientation of $CuInS_2$ in the (112) plane.

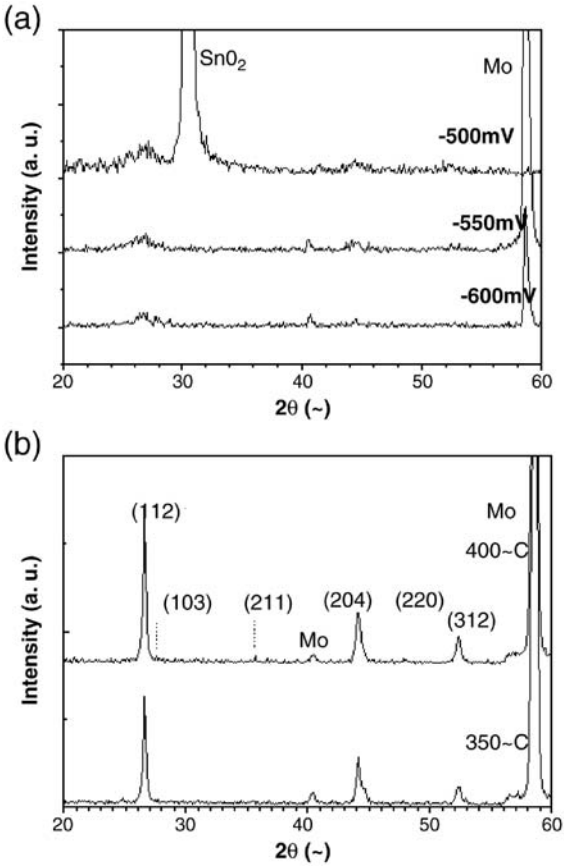

Fig. 6. a: XRD patterns of as-electrodeposited CISe film at −500, −550 and −600 mV vs. SCE. b: XRD patterns of electrodeposited CISe films annealed at 350 and 400 °C in vacuum.

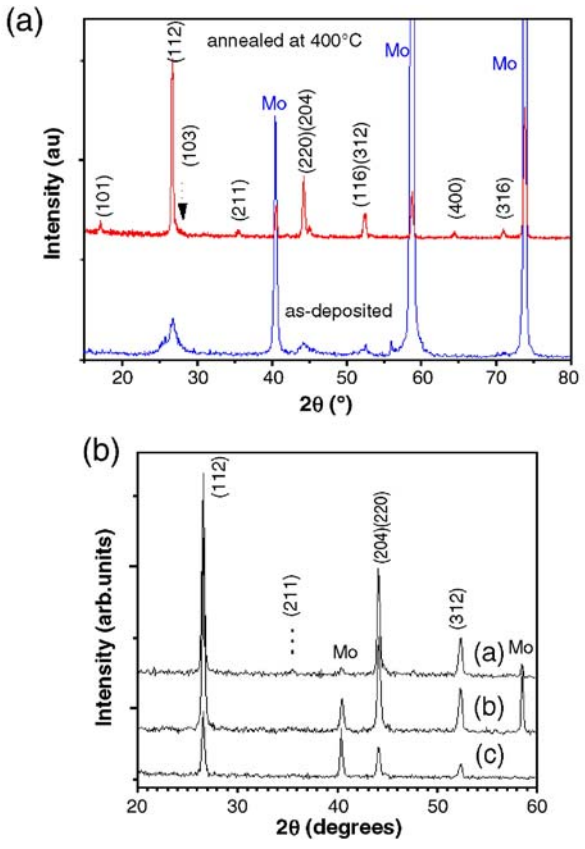

Fig. 7. a: XRD patterns of CIGSe films before and after annealing at 400 °C in vacuum. b: XRD patterns of $CuIn_{1-x}Ga_xSe_2$ films annealed at 400 °C in vacuum, prepared at different concentrations of $Ga_2(SO_4)_3$ in solution: a) 0.5 mM, b) 1.12 mM and c) 1.4 mM.

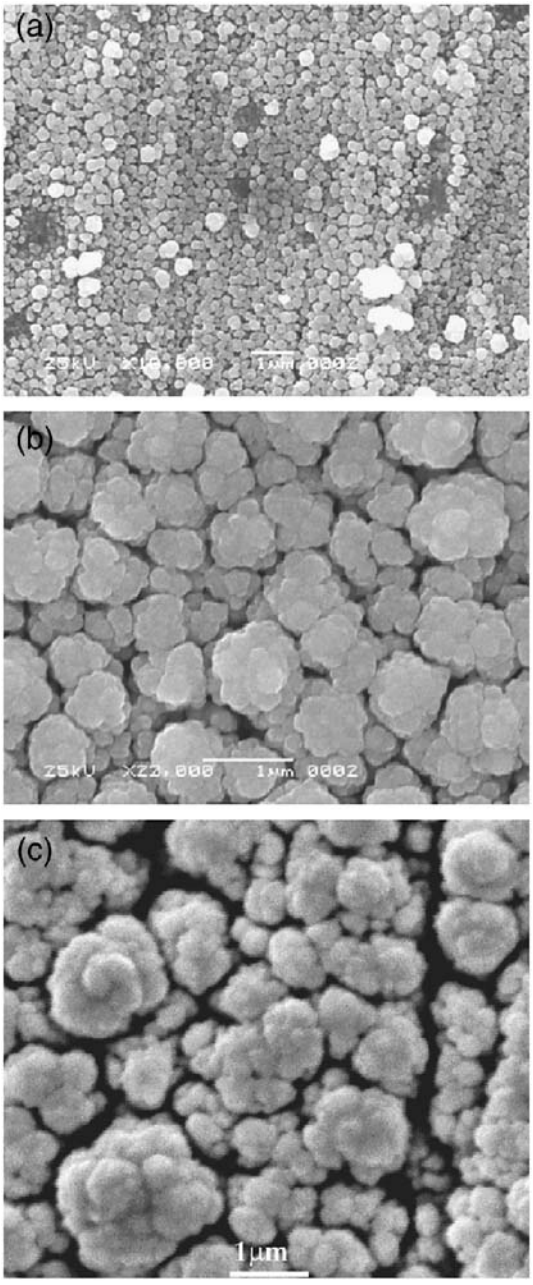

Fig. 8. SEM micrographs of: a) as-deposited CISe film, b) annealed CISe film at 400 °C in vacuum, c) annealed CIGSe film at 400 °C in vacuum.

SEM micrograph of the chalcogenised sample at 400 °C is shown in Fig. 3. The film consists of a compact morphology and homogeneous grains. The size of the crystallites is less than 1 μm.

Optical measurements have shown that our films are highly absorbing. The absorption coefficients measured are higher than 10^4 cm^{-1}. The band gap value deduced from the optical spectra (Fig. 4) indicates a value of about 1.43 eV in good agreement with the results published in the literature.

3.2. Electrodeposited CISe and CIGSe

Typical voltamograms during the one step electrodeposition of CISe and CIGSe thin films are shown in Fig. 5. The bath consisted in the solution: $CuSO_4$ (3 mM), $In_2(SO_4)_3$ (3 mM) and SeO_2 (5 mM) without $Ga_2(SO_4)_3$ (Curve a) and with a 1.5 mM of $Ga_2(SO_4)_3$ solution. The codeposition of Cu, In, Se and Ga occurs in the potential range between −350 to −700 mV vs. SCE (Satured Calomel Electrode). All the results reported here were prepared at the potential between −500 and −700 mV vs. SCE. Fig. 6a and b compare the XRD spectra of the as-deposited CISe films and after annealing in vacuum at 350 and 400 °C. The as-deposited films are almost amorphous. Annealing in vacuum has led to the formation of the well known chalcopyrite structure of $CuInSe_2$ with the preferential orientation in the (112) plane. The crystallite size as determined using Sherrer's formula from the half width of the (112) peak is larger than 40 nm.

Fig. 7 shows the XRD spectra of CIGSe samples prepared at a potential −500 mV after annealing at 400 °C in vacuum for 1 h. This figure illustrates the influence of the Ga content in the films. First, we point out the formation of the chalcopyrite structure with the preferential orientation in the (112) plane (Fig. 7a). However, a net decrease in the intensity of the peaks is shown upon increasing the $Ga_2(SO_4)_3$ concentration (Fig. 7b). This may be attributed to incorporation of Ga in the In sites leading to the distortion of the lattice [11] in agreement with the results reported by other authors concerned with electrodeposited CIGSe using $GaCl_3$ as Ga precursor [24,25]. EDS analysis has shown that the Ga content in our films increases with the $Ga_2(SO_4)_3$ concentration as reported in our previous work [11].

Fig. 8 compares the SEM micrographs of the as-deposited film and after annealing at 400 °C with and without Ga. The as-deposited CISe film consists in clusters of small grains. For the annealed films, the micrographs show, for both CISe and CIGSe films, a more homogeneous distribution of grains and compact morphology. The grain size for this film is higher than 0.5 μm. The grains seem to be made of clusters of nanoparticles in good agreement with XRD analysis that has shown that the grain size is about 40 nm.

Optical measurements show that all the films exhibit a high absorption coefficient of about 10^5 cm^{-1}. Similar values were reported for $CuInSe_2$ films prepared by vacuum method [26]. Such value is higher than those measured on our $CuInS_2$ films prepared by sputtering. Fig. 9 shows the variation of the $(\alpha h\upsilon)^2$

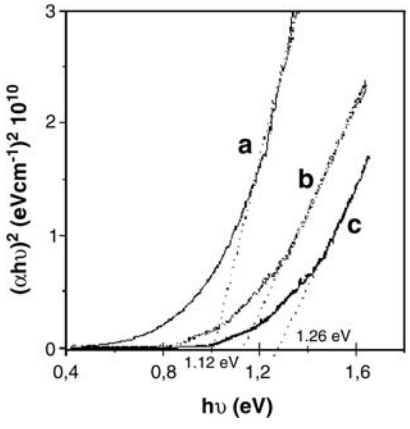

Fig. 9. Plots of $(\alpha h\upsilon)^2$ versus $h\upsilon$ for $CuIn_{1-x}Ga_xSe_2$ films prepared with different compositions: a) $x=0$, b) $x=0.18$ and c) $x=0.23$.

as a function of the energy for the $CuIn_{1-x}Ga_xSe_2$ films. The band gap value increases with Ga content from 1.01 eV for CISe to 1.26 eV for $x=0.23$. The maximum Ga content in our film is about 6%. Unfortunately, we couldn't explain the mechanism responsible for limited Ga incorporation in our films. Up to now, serious interpretation of gallium electrochemical insertion phenomenon is lacking at our knowledge.

Finally, the resistivity of our films was adjusted to 10 Ωcm by appropriate heat treatments as described in our previous work [11].

4. Conclusion

CI(S,Se) and CIGSe thin films were successfully prepared by both a vacuum and a non-vacuum methods. All the films crystallize in the well known chalcopyrite structure with the preferential orientation in the (112) plane. The most important conclusion pointed out after this study is that electrodeposition is an interesting and cost effective technique for the preparation of good quality CISe and CIGSe films. The Ga grading could be performed by the simple addition of gallium precursor in the deposition solution. It is appropriate for large area processing and thus could constitute a viable and promising option to low-cost solar energy production as expected by the results obtained in the framework of the CISEL project [12,27].

Acknowledgments

This work was partially supported by the CNRST/CNRS cooperation program (Chimie 05/06).

References

[1] K. Ramanathan, M.A. Contreras, C.L. Perkins, S. Asher, F.S. Hasoon, J. Keane, D. Young, M. Romero, W. Metzger, R. Noufi, J. Ward, A. Duda, Prog. Photovolt. Res. Appl. 11 (2003) 225.
[2] M.A. Contreras, K. Ramanathan, J. Abushama, F.S. Hasoon, D.L. Young, B. Egaas, R. Noufi, Prog. Photovolt. Res. Appl. 13 (2005) 209.
[3] M.A. Contreras, B. Egaas, K. Ramanathan, G. Hiltner, A. Swartzlander, F. Hasoon, R. Noufi, Prog. Photovolt. 7 (1999) 311.
[4] M. Powalla, B. Dimmler, R. Chaeffler, G. Woorwenden, U. Stein, H.-D. Mohring, F. Kessler, D. Hariskos, Proc. 19th European Photovoltaic Solar Energy Conference and Exhibition, Paris, France, June 11–15, 2004, p. 1663.
[5] M. Yamagushi, J. Appl. Phys. 78 (1995) 1476.
[6] L. Solt, J. Hedstrom, J. Kessler, M. Ruckh, K.O. Velthaus, H.W. Schock, Appl. Phys. Lett. 62 (1993) 597.
[7] M.A. Gabor, J.R. Tuttle, D.S. Albin, M.A. Contreras, R. Noufi, A.H. Herman, Appl. Phys. Lett. 65 (1994) 198.
[8] A. Gupta, S. Isomura, Sol. Energy Mater. Sol. Cells 53 (1998) 385.
[9] T. Pisarkiewicz, H. Jankowski, E. Schabowska-Osiowska, L.J. Maksymovicz, Opto-Electron. Rev. 11 (2003) 297.
[10] S. Nishiwaki, T. Satoh, S. Hayashi, Y. Hashimoto, S. Shimakawa, T. Negami, T. Wada, Sol. Energy Mater. Sol. Cells 67 (2001) 217.
[11] K. Bouabid, A. Ihlal, A. Manar, A. Outzourhit, E.L. Ameziane, Thin Solid Films 488 (2005) 62.
[12] S. Taunier, J. Sicx-Kurdi, P.P. Grand, A. Chomont, O. Ramdani, L. Parissi, P. Panheleux, N. Naghavi, C. Hubert, M. BenFarah, J.P. Fauvarque, J. Connolly, O. Roussel, P. Mogensen, E. Mahe, J.F. Guillemoles, D. Lincot, O. Kerrec, Thin Solid Films 480/481 (2005) 526.
[13] D. Lincot, J.F. Guillemoles, S. Taunier, D. Guimard, J. Sicx-Kurdi, A. Chaumont, O. Roussel, O. Ramdani, C. Hubert, J.P. Fauvarque, N. Bodreau, L. Parissi, P. Panheleux, P. Fanouillere, N. Naghavi, P.P. Grand, M. BenFarah, P. Mogensen, O. Kerrec, Sol. Energy 77 (2004) 725.
[14] A. Ennaoui, M. Bar, J. Klaer, T. Kropp, R. Saez-Araoz, M.Ch. Lux-Steiner, Prog. Photovolt. Res. Appl. 14 (2006) 499.
[15] A. Ennaoui, W. Eisele, M. Lux-Steiner, T.P. Niesen, F. Karg, Thin Solid Films 431/432 (2003) 335.
[16] C.H. Huang, S.S. Li, W.N. Shafarman, C.H. Chang, E.S. Lambers, L. Rieth, J.W. Johnson, S. Kim, B.J. Stanbery, T.J. Anderson, P.H. Holloway, Sol. Energy Mater. Sol. Cells 69 (2001) 131.
[17] T. Nakada, K. Kurumi, A. Kunioka, IEEE Trans. Electron Devices 46 (1999) 2093.
[18] S. Spiering, D. Hariskos, M. Powalla, D. Lincot, Thin Solid Films 431/432 (2003) 359.
[19] A. Ihlal, K. Bouabid, D. Soubane, O. Ait-Taleb-Ali, M. Nya, A. Outzourhist, G. Nouet, Proc. of the 20th European photovoltaic solar energy conference, Barcelone, Spain, June 6–10, 2005, p. 1783.
[20] K. Bouabid, A. Ihlal, A. Manar, A. Sdaq, A. Outzourhit, E.L. Ameziane, J. Phys., IV 123 (2005) 47.
[21] K. Bouabid, A. Ihlal, A. Manar, A. Outzourhit, E.L. Ameziane, J. Phys., IV 123 (2005) 53.
[22] K.A. Lindahl, J.J. Moore, D.L. Olson, R. Noufi, B. Lanning, Thin Solid Films 290–291 (1996) 518.
[23] Y. Yamamoto, T. Yamagushi, Y. Demizu, T. Tanaka, Thin Solid Films 281/282 (1996) 372.
[24] M.E. Calixo, R.N. Bhattacharya, P.J. Sebastian, A.M. Fernandez, S.A. Gamboa, R. Noufi, Sol. Energy Mater. Sol. Cells 55 (1998) 23.
[25] P.J. Sebastian, M.E. Calixo, R.N. Bhattacharya, R. Noufi, Sol. Energy Mater. Sol. Cells 59 (1999) 125.
[26] L.L. Kamerski, M. Hallerdt, P.J. Irland, R.A. Hickelsen, W.S. Chen, J. Vac. Sci. Technol., A 1 (1983) 395.
[27] J. Kessler, J. Sicx-Kurdi, N. Naghavi, J.-F. Guillemotes, D. Lincot, O. Kerrec, M. Lamirand, L. Legras, P. Mogensen, Proc. of the 20th European photovoltaic solar energy conference, Barcelone, Spain, June 6–10, 2005, p. 1704.